RSC Advances

PAPER

View Article Online
View Journal | View Issue

Cite this: *RSC Adv.*, 2020, **10**, 1388

Effective multi-metal removal from plant incineration ash *via* the combination of bioleaching and brine leaching

Su Li,†[ab] Zhuang Tian,†[ab] Ronghui Liu,[ab] Wenbo Zhou,[ab] Haina Cheng,[ab] Jianxing Sun,[ab] Kaifang Zhao,[c] Yuguang Wang*[ab] and Hongbo Zhou*[ab]

Plant incineration ash is the final product from the remediation of multi-metal contaminated soils by the phytoextraction process. The content of heavy metals in plant ash was found to be higher than the regulatory criteria and it was thus classified as hazardous waste. So far, no eco-friendly and cost-effective technology has been developed for the management of this residue. Herein, a cleaner strategy of bioleaching combined with brine leaching of multi-metals from plant ash was developed. The bioleaching results indicated that 88.7% (Zn), 93.2% (Cd), 99.9% (Mn) and 13.8% (Pb) were achieved under optimum conditions of Fe(II) concentration 6.0 g L^{-1}, pH 1.8 and pulp density 15% (w/v). Subsequently, the introduction of brine leaching using 200 g L^{-1} NaCl significantly increased Pb recovery to 70.6% under conditions of 15% (w/v) pulp density, thereby ultimately achieving deep recovery of all metals. An investigation of the mechanism revealed that H^+ attack and microorganisms were the dominant mechanism for bioleaching of Zn, Cd and Mn, and the bioleaching kinetics of Zn in ash were controlled by interface mass transfer and diffusion across the product layer. Risk assessment tests indicated that the leached residues could pass the TCLP test standard and be safely reused as nonhazardous materials. These findings demonstrated that the two-stage leaching strategy was feasible and promising for multi-metal removal from plant ash.

Received 10th October 2019
Accepted 30th October 2019

DOI: 10.1039/c9ra08267k

rsc.li/rsc-advances

1 Introduction

Phytoextraction has been widely employed in remediating soils contaminated with heavy metals,[1] but this technology discharges large volumes of heavy metal-enriched plant biomass (HMEPB). Incineration is recognized to be the best method of waste disposal with more than 90% biomass reduction.[2,3] However, incineration of HMEPB raises new challenges for waste disposal of the plant incineration ash generated. About 10% bottom ash with mass accumulation of various toxic heavy metals is produced,[4] containing Zn, Cd, Mn, Pb, *etc.*[5–7] Moreover, the content of heavy metals in plant ash was found to be higher than the regulatory criteria and it can be classified as hazardous waste.[8,9] Besides, deep recovery of heavy metals from the ash is the key to substantial utilization of ash. Therefore, to avoid threats to the environment and limiting the applications for reuse,[9] it is highly necessary to recycle the metals present in the ash.

In general, for metal removal, special measures, such as high acidity, high temperature and high pressure, should be taken.[10] In recent years, metal removal strategies for fly ash or bottom ash have involved solidification/stabilization,[11] thermal treatment,[12] supercritical fluid extraction,[13] acid/alkali leaching,[14] *etc.* However, supercritical fluid extraction, thermal treatment and acid leaching suffer from the main disadvantages of high cost, high energy consumption and secondary pollution, respectively. Besides, solidification/stabilization could utilize cementitious material to solidify the harmful substance to meet the requirements for admission to landfill. However, on the one hand, the volume and mass of waste would increase after solidification. On the other hand, under various special conditions (for example, an acid environment), the harmful metals in treated waste can easily leak out, which poses a potential threat to the environment and human health, thus limiting the possibility of reuse.

However, up to now, the characteristic of plant ash have been unclear and the strategy to recover metals from the ash has not been extensively addressed. Giving the same importance to environmental protection and resource recovery, a clear strategy for deep recovery of the metals is urgently required. Bioleaching, as a low-cost and low-energy 'green technology', is a suitable alternative method to treat solid waste, and different metals are more easily recovered from

[a]*School of Minerals Processing and Bioengineering, Central South University, Changsha, Hunan, 410083, China. E-mail: zhouhb@csu.edu.cn; ygwang@csu.edu.cn*
[b]*Key Laboratory of Biometallurgy of Ministry of Education, Central South University, Changsha 410083, China*
[c]*Dongguan Kecheng Environmental Technology Co., Ltd., Dongguan 523899, China*
† Su Li and Zhuang Tian are co-first authors.

bioleached residues or leachate.[15] Bioleaching mainly uses various microbes to dissolve metals, including acidophilic chemoautotrophic or heterotrophic bacteria or fungi. To date, bioleaching has been successfully employed to extract metals from sewage sludge, electronic waste, mine tailings *etc*[16–18]. However, bioleaching of solid wastes is still not a very mature method because of its slow kinetics and poor dissolution,[19] and it needs further process optimization. Then, as regards its complexity and the diversity of solid wastes, our knowledge about the application of bioleaching with an acidophilic iron-oxidizing consortium for extracting multi-metals from plant ash is limited.[20,21] In addition, bioleaching cannot efficiently remove the toxic heavy metal Pb but it can enrich Pb in the form of semi-soluble lead sulfate ($K_{sp} = 1.8 \times 10^{-8}$).[17] For deep Pb recovery, a process to improve lead recovery after biological enhancement is necessary. Studies indicated that brine leaching is the most recognized and widely used recovery method.[22] However, there are limited reports focusing on lead removal from bioleached residue. Therefore, the combination of bioleaching and brine leaching for multi-metal removal from plant ash is worth evaluating.

In this study, an adapted iron-oxidizing consortium was constructed and employed in the bioleaching system. We firstly investigated the effects of ferrous iron, pH and pulp density on bioleaching metals from plant ash. Then the residues were subjected to brine leaching to remove further Pb and the optimum leaching conditions were investigated. Moreover, the mechanism for the release of metals in bioleaching processes was explored. Finally, environmental risk evaluation tests for plant ash were conducted. Based on these results, a clever two-stage leaching strategy was proposed to extract multi-metals from plant ash in this experiment.

2 Material and methods

2.1 The plant ash

The plant ash used in this study was obtained from Shaoguan in Guangdong province (China). Prior to use, the ash was dried at room temperature to constant weight, ground in a ball mill, and sieved through a 200 mesh (≤75 μm). The characteristics of the plant ash were determined by ICP-OES, XRD, SEM and FTIR. The toxicity characteristics of the ash were evaluated with the Toxicity Characteristic Leaching Procedure (TCLP: USA). To analyze the metal contents in the plant ash, *aqua regia* (volume ratio of HCl to $HNO_3 = 3:1$) was used to dissolve the materials fully. The distribution of species of heavy metals in the raw plant ash was analyzed by a modified European Community Bureau of Reference (BCR) sequential extraction procedure.

2.2 Adaptation of acidophilic iron-oxidizing consortium

A mixed microbial consortium, comprising three species of iron-oxidizing acidophiles, *Leptospirillum ferriphilum*, *Ferroplasma thermophilum* and *Sulfobacillus thermosulfidooxidans* (stored in our laboratory), was used as the inoculum for subsequent adaption. The iron-oxidizing consortium was inoculated (10%, v/v) into 90 mL of 9 K medium supplemented with $FeSO_4 \cdot 7H_2O$ (44.7 g L^{-1}) as energy substrate and incubated on a rotary incubator shaker at 30 °C in a 250 mL Erlenmeyer flask. Modified 9 K medium (g L^{-1}): $(NH_4)_2SO_4$ (3.0), $MgSO_4 \cdot 7H_2O$ (0.5), K_2HPO_4 (0.05), KCl (0.1), $Ca(NO_3)_2$ (0.01).[23] After that, the consortium was acclimated to gradually increasing pulp densities of plant ash (10%, w/v), as described in previous studies.[24] The medium pH was initially adjusted to 2.0 with H_2SO_4 (50%, v/v).

2.3 Bioleaching experiments

The bioleaching experiments were carried out in 1 L stirred tank reactors (0.5 L working volume, 350 rpm, 30 °C, 12 h). And a two-step bioleaching strategy was adopted, as described by previous studies.[25] Briefly, the biogenic lixiviant was collected from the adapted microbial cultures during the logarithmic phase of the growth curve and the plant ash was then added to the biogenic ferric solution. During bioleaching, the effects of Fe(II) concentration (3.0–9.0 g L^{-1}) on bioleaching behavior were investigated and the pH and pulp density were controlled at 2.0 and 10% (w/v), respectively. Secondly, to determine the effects of pH, bioleaching tests were carried out at various pH values (1.3–2.5) with an optimum Fe(II) concentration and 10% (w/v) pulp density. Finally, the effects of pulp density (5–30%) on metal release in plant ash were studied based on the first and second series of experiments. Thereafter, the properties of the bioleaching residues were analyzed under optimal conditions based on the above results, in order to further investigate the bioleaching behavior. Control tests were also conducted by directly adding Fe(III) (6.0 g L^{-1}). The pH of the solution was controlled by the addition of sulfuric acid during the bioleaching process. All experiments were carried out in triplicate, and evaporation of water was compensated for with distilled water. Samples were withdrawn at regular intervals to analyze the concentrations of the metals.

2.4 Brine (NaCl) leaching experiments

As Pb(II) dissolved into solution after bioleaching would form semi-soluble $PbSO_4$ and remain in the bioleached residues, the brine leaching was then employed for further recycling of Pb from the bioleached residues. The experiments were performed in 0.5 L stirred reactors with 100 mL working volume. The effects of NaCl concentration (50–250 g L^{-1}) and pulp density (5–30%, w/v) were successively investigated to achieve maximum Pb leaching. The other leaching conditions were as follows: 200 rpm, pH 1.2 and 30 °C. All the experiments were performed in triplicate.

2.5 Analytical methods

(1) The physicochemical analysis: the pH of the plant ash was measured with a pH S-3C acid meter (INESA Scientific Instrument Co. Ltd, China) after adding distilled water in the ratio of 1 : 10 (w/v). The ORP (oxidation–reduction potential) of the bioleaching system was measured with a Pt *vs.* Ag/AgCl

potential electrode. Solid samples were characterized by a Fourier Transform Infrared Spectrometer (FT-IR, Thermo Fisher Nicolet 6700), X-ray Diffractometer (XRD, Rigaku Ultima-III) and Scanning Electron Microscope (SEM, Quanta 250). The concentrations of metals in the solutions were determined with an inductively coupled plasma-optical emission spectrometer ICP-AES (Optima 5300 DV, PerkinElmer instrument).

(2) Modified BCR sequential extraction procedure: a BCR (Community Bureau of Reference) sequential extraction procedure was used to describe the metal speciation and obtain exchangeable, reducible, oxidizable and residual fractions.[26] The extraction procedures were displayed as follows: ① exchangeable fraction: 20 mL of 0.11 M HOA per 0.5 g of dry ash was shaken for 16 h at 25 °C; ② reducible fraction: 20 mL of 0.5 M $NH_2OH{\cdot}HCl$ (pH = 2.0) was added to the residue and shaken for 16 h at 25 °C; ③ oxidizable fraction: 5 mL of 8.8 M H_2O_2 was added to the residue and digested for 1 h at 25 °C, and then for 1 h at 85 °C in a water bath with a second volume of H_2O_2. Then, the solution was evaporated to about 1 mL. 25 mL of 1 M NH_4OAc (pH 2.0) was added to the residue and shaken for 16 h at 25 °C; ④ residual fraction: HNO_3–HF–$HClO_4$ digestion, using the same procedure as for the total metal determination.

(3) Toxicity analysis: the toxicities of the raw dried ash and leaching residues were evaluated by a TCLP test according to the US Environmental Protection Agency 1311 Test Toxicity Characteristic Leaching Procedure.[27] Briefly, samples were mixed with buffered acetic acid at a pH of 4.99 in a solid to liquid ratio of 1 : 20, and after stirring at 32 rpm and being kept at 22.5 °C for 18 h, samples of leachate were collected and filtered with a glass fiber filter (0.8 mm) for metal content determination.

(4) Concentrations of Cd, Mn, Zn, Pb and total iron in the leachates were determined by an inductively coupled plasma-optical emission spectrometer (ICP-OES) (Optima 5300 DV, PerkinElmer instrument). The leaching rate can be calculated using the following equation:

$$\mathrm{ER}(\%) = \frac{C \times V}{m \times \alpha} \times 100$$

where ER represents the leaching rate of metals; C is the content of metals in solution; V is the solution volume; α is the content of metals in the dried sample; m is the mass of the sample. During calculations, the mean values of three parallel experimental results were taken as the results.

3 Results and discussion

3.1 Characteristics of plant ash

The metal contents in dried plant ash are shown in Table 1. According to the Soil Environmental Quality Standard implemented in China (GB/15618/2018), Table 1 indicated that the heavy metals in raw plant ash exceeded the criterion to various degrees: three times Mn, 10 times Zn and Cd, twice Pb. The XRD pattern in Fig. 7a showed that the raw plant ash mainly contained three primary crystalline phases: SiO_2, KCl and $CaCO_3$, indicating that the heavy metals Mn, Pb, Zn, Cd and Fe in the dried ash were present as amorphous forms. The metal fractions obtained by the BCR analysis showed that the oxidizable fraction accounted for the percentage of content for Mn, Zn, Cd and Pb with 80.06%, 73.40%, 57.02% and 81.47%. Besides, it was found from the toxicity analysis in Table 4 that Zn, Cd, Mn, Cr and Ni in the leachate are much higher than the Chinese regulatory limit (Chinese National Standard, GB8978-1996). Accordingly, the plant ash should be categorized as hazardous waste. Overall, these results reflected that the properties of the plant ash were significantly different from those previously reported for fly ash. Therefore, a suitable new strategy for cleanup of the plant ash is urgently required before landfilling or reuse.

Table 1 Physical and chemical properties of plant ash

Item	Plant ash (mg kg^{-1})	Risk value[b] (mg kg^{-1})
pH[a]	10.48 ± 0.30	—
Mn	3888.0 ± 60.3	—
Zn	2278.0 ± 52.3	200
Cd	5.1 ± 0.4	0.3
Pb	187.9 ± 6.3	80
Cr	28.0 ± 1.3	250
Cu	86.6 ± 4.4	50
Ni	81.5 ± 3.1	60
Fe	13 360.0 ± 230.9	—
K	15 300.0 ± 100.6	—
Ca	42 170.0 ± 401.8	—
Na	937.0 ± 16.1	—
Cl	980.0 ± 19.5	—

[a] The pH value: based on Chinese Standard of Solid Waste – Glass Electrode Test Method of Corrosivity (GB/T 15555.12-1995). [b] The risk value referred to Soil environmental quality – Risk control standard for soil contaminated of agricultural land of China (GB 15618-2018).

3.2 Effects of Fe(II) concentration on bioleaching of multi-metals

During bioleaching, it is suggested that Fe(II) as the energy substrate of the iron-oxidizing consortium is vital in metal extraction. The effects of different Fe(II) concentrations (3.0–9.0 g L^{-1}) on metal removal are shown in Fig. 1. It was found that Zn, Cd and Mn extraction at 3.0 g L^{-1} and 9.0 g L^{-1} Fe(II) were both significantly lower than that when the Fe(II) concentration was 4.5 or 6.0 g L^{-1} (t-test, $p < 0.05$). This may be due to the release of metals being slow under conditions of a low concentration of Fe(II) and the formation of passivation layer with a high concentration of Fe(II). However, the redox potential of all systems eventually tends to be about 550 ± 20 mV (Fig. 1(e)).

To sum up, an increase in Fe(II) energy addition promoted the leaching of heavy metals from the plant ash and reduced the total consumption of H_2SO_4 (Fig. 1(f)), which is consistent with previous studies.[28] The acidophilic iron-oxidizing consortium could convert Fe(II) to Fe(III) within a certain pH range (1.0–2.5) (eqn (1)). But an excessively high concentration of iron is unstable, and can easily form the secondary mineral jarosite

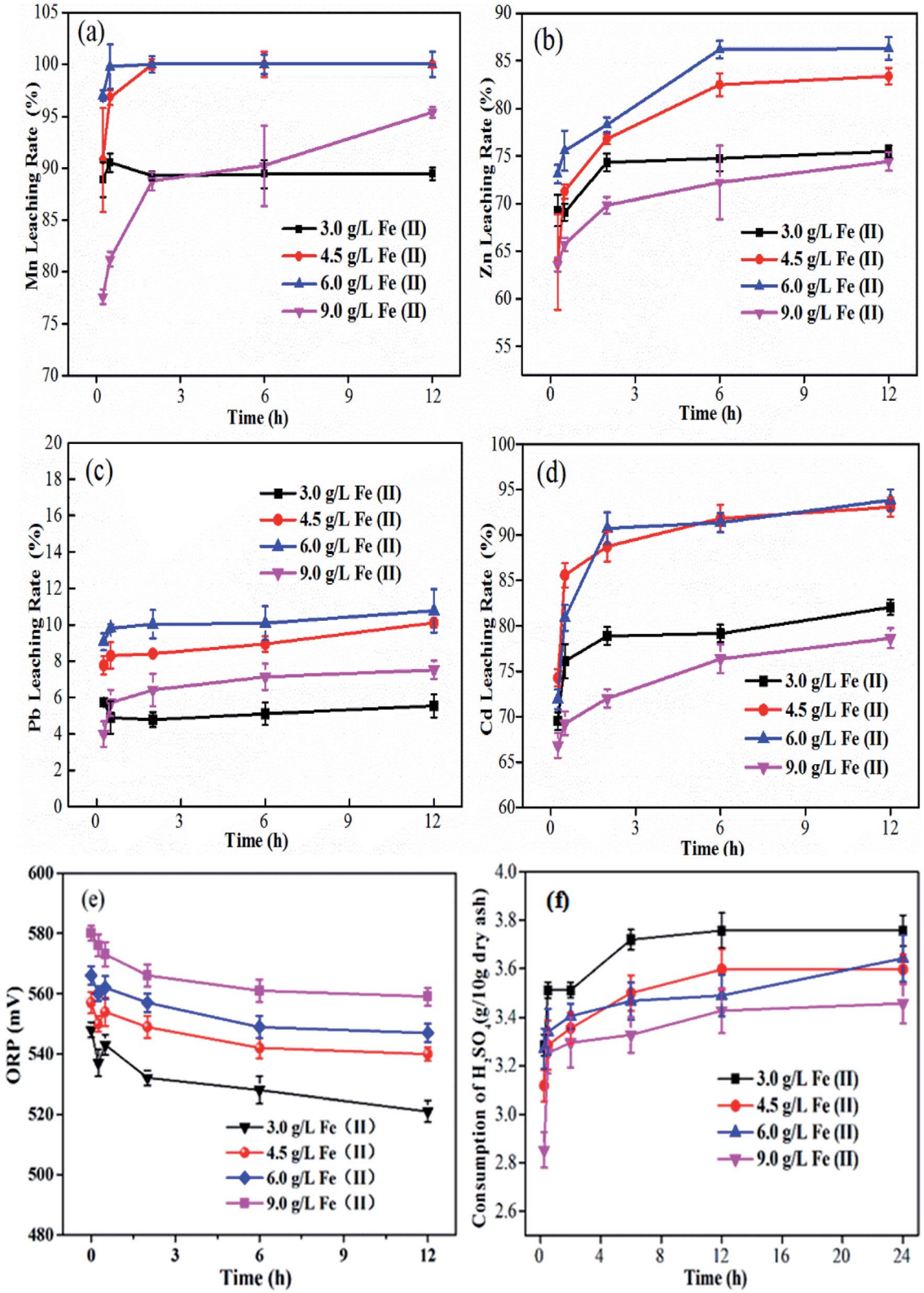

Fig. 1 Variations in bioleaching rates of Mn (a), Zn (b), Pb (c), Cd (d); the redox potential (e) and the total H_2SO_4 consumption (f) over time with different Fe(II) concentrations.

and other precipitates. Jarosite precipitation can also lead to the co-precipitation of metals (Zn, Cu, Ni, *etc.*) (eqn (2)–(5)).[28] Therefore, considering the metal release and the cost of acid consumption, an Fe(II) concentration of 6 g L^{-1} was selected for the following studies. And the reactions during bioleaching process could be described by eqn (1)–(5):

$$4Fe^{2+} + O_2 + 4H^+ \rightarrow 2Fe^{3+} + 2H_2O \quad (1)$$

$$MO + 2H^+ \rightarrow M^{2+} + H_2O \quad (2)$$

$$MCO_3 + 2H^+ \rightarrow M^{2+} + H_2O + CO_2 \quad (3)$$

$$M^x + yFe^{3+} \rightarrow yFe^{2+} + M^{(x+y)+} \quad (4)$$

$$6Fe^{3+} + 12H_2O + 2A^+ + 4SO_4^{2-} \rightarrow 2AFe_3(SO_4)_2(OH)_6\downarrow + 12H^+ \quad (5)$$

where $A^+ = K^+$, Na^+, NH_4^+; and M = Mn, Zn, Cd, Pb.

3.3 Effects of pH on bioleaching of multi-metals

It is well known that pH is an important parameter in bioleaching using acidophiles.[29,30] In conditions of 6.0 g L^{-1} Fe(II) and 10% (w/v) pulp density, the leaching behaviors of Zn, Cd, Mn and Pb during the bioleaching process with different pH values are displayed in Fig. 2. It was found that the leaching efficiencies of Zn and Cr increased remarkably as the pH value decreased from 2.5 to 1.8, owing to the quick reaction between the high H^+ concentration and the metals. After 12 hours at a pH of 1.8, the extraction rate of Zn is up to 89.5%. Additionally, the maximum removal of Cd (96.7%) was obtained at pH 2.0 within 12 h while there was not much difference at the end of runs at pH 1.8–2.0. A different pattern was observed for Pb extraction of around 10%, which was relatively less affected by different pH values. It was also found that almost 100% of Mn was extracted within 2 h with a pH between 1.3 and 2.5.

The processing pH, controlled by the addition of sulfuric acid during bioleaching, can provide proton attack for the target metal dissolution[31] and avoid the precipitation of iron that took place when the pH was ≥2.5.[30] During the process of biomass accumulation of the acidophilic iron-oxidizing consortium,

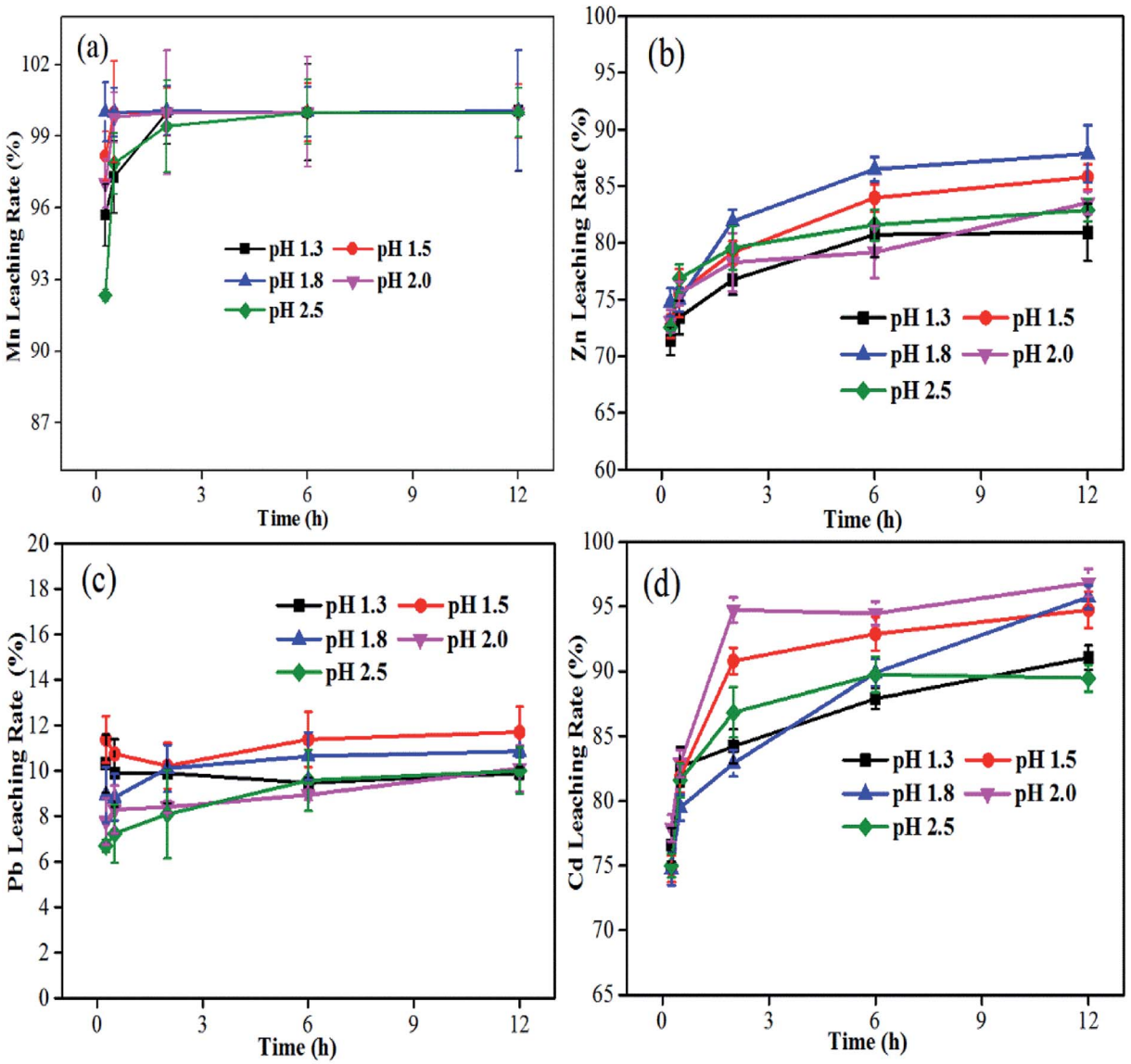

Fig. 2 Variations in bioleaching rates of Mn (a), Zn (b), Pb (c) and Cd (d) over time with different pH values.

Fe(II) would be oxidized to Fe(III), resulting in a rise in pH which would require an increase in acid consumption to control. To maximize metal recovery and reduce acid consumption, controlling pH in a proper range is necessary. In the present study, it is appropriate to operate the bioleaching at pH 1.8 for the selective co-dissolution of Zn and Cd.

A further increase in pulp density to 20–30% would lead to a larger decrease in the dissolution of Mn, Zn and Cd. This may be due to a reduction in dissolved oxygen and limitation of mass transfer, resulting in a promotion of Fe(III) precipitation.[32] However, metal leaching at a pulp density ≤15% was less affected. Therefore, 15% (w/v) of high pulp density was recommended for bioleaching in plant ash.

3.4 Effects of pulp density on bioleaching of multi-metals

A high pulp density has negative effects on bioleaching efficiency, while a high pulp density is always preferable for industrial applications.[32] The effects of pulp density are indicated in Fig. 3. Different pulp densities have little effect on lead leaching with a removal rate of around 10%. Similarly, a slight fluctuation in Mn removal (100–98.1%) was observed from 5% to 15% (w/v) pulp density after 12 h of bioleaching. In addition, with the increase in pulp density (5–15% (w/v)), the leaching rates for Zn and Cd both decreased, from 92.0% and 97.4% to 87.9% and 92.8%, respectively. In comparison with previous studies which performed the bioleaching of MSW incinerator fly ash at a pulp density of 1–2%,[33] the current work obtained more than 99.9% of Mn, 88.7% of Zn, 93.2% of Cd at a high pulp density of 15% (w/v) and which were extracted at an optimum pH of 1.8 and Fe^{2+} concentration of 6.0 g L^{-1}.

3.5 Brine leaching Pb from bioleached residues

After bioleaching under optimal conditions, the recovery of Pb was still very low (only 13.8%) due to the formation of a large amount of $PbSO_4$, which is insoluble in water, but soluble in saturated chloride solutions acidified by HCl or H_2SO_4. To further remove Pb from bioleached residues, brine (NaCl) leaching was employed to treat bioleached residues, and the effects of NaCl concentration and pulp density were investigated. It can be observed from Fig. 5a that lead recovery increased significantly when the NaCl concentration increased from 50 to 200 g L^{-1}. The maximum lead extraction (72.5%) was obtained at 200 g L^{-1} NaCl. In conditions of low NaCl concentration, SO_4^{2-} in bioleached residues and Cl^- in solution can take the form of $PbCl_2$, which has a solubility of 9.9 g L^{-1} (at room temperature) (eqn (6)). With an increase in Cl^- concentrations to 200 g L^{-1}, $PbCl_2$ is subsequently converted to more

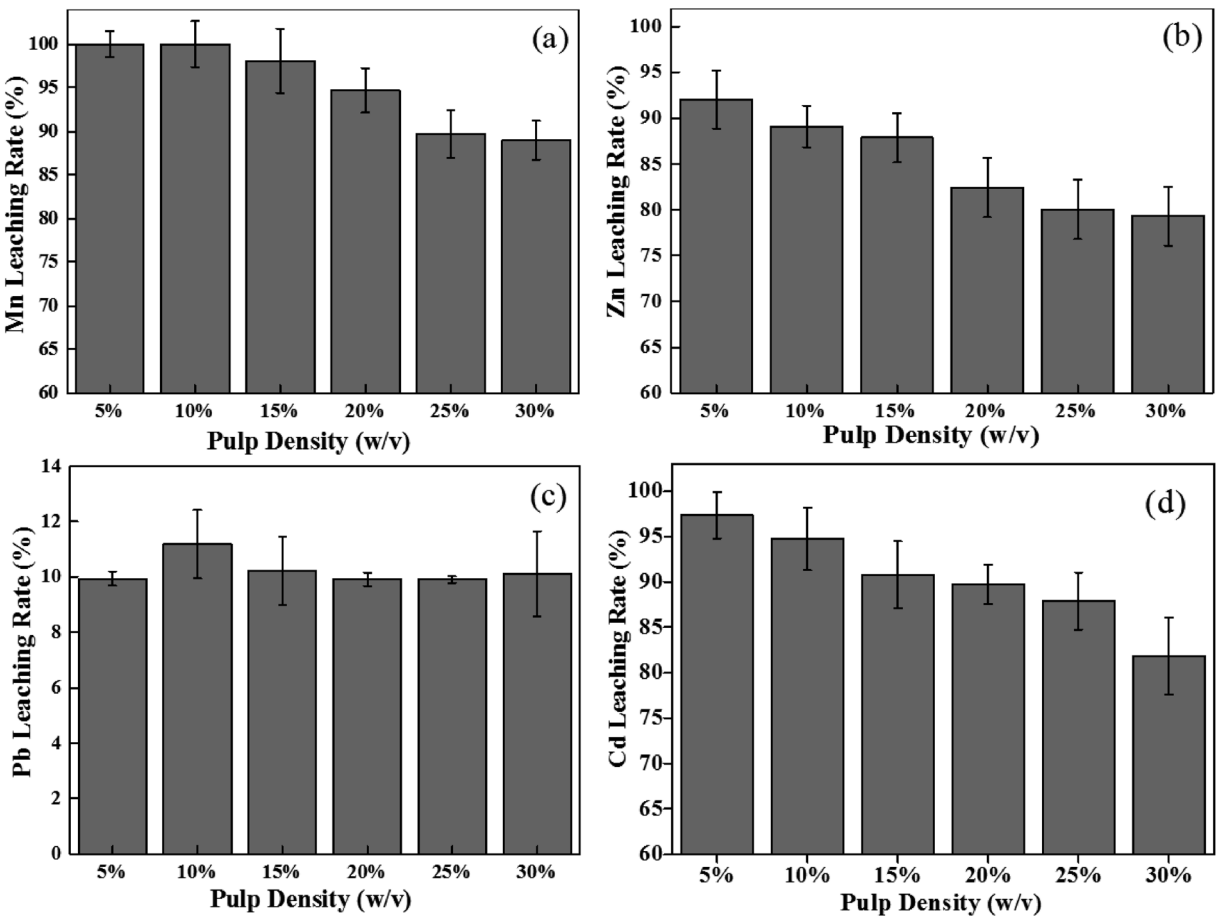

Fig. 3 Effects of different pulp densities on bioleaching rate of Mn (a), Zn (b), Pb (c) and Cd (d) at 12 h.

and more soluble complexes of $PbCl^{3-}$ and $PbCl_4^{2-}$ (eqn (7) and (8)).[34] However, once NaCl exceeded the saturated chloride concentration of 200 g L^{-1}, lead recovery greatly decreased, which may be related to the formation of sodium jarosite.[35] During brine leaching, lead forms complex ions in concentrated chlorine solutions based on the following expressions:

$$PbSO_4(s) + 2Cl^- \rightleftharpoons PbCl_2(s) + SO_4^{2-} \quad (6)$$

$$PbCl_2 + Cl^- \rightleftharpoons PbCl_3^- \quad (7)$$

$$PbCl_3^- + Cl^- \rightleftharpoons PbCl_4^{2-} \quad (8)$$

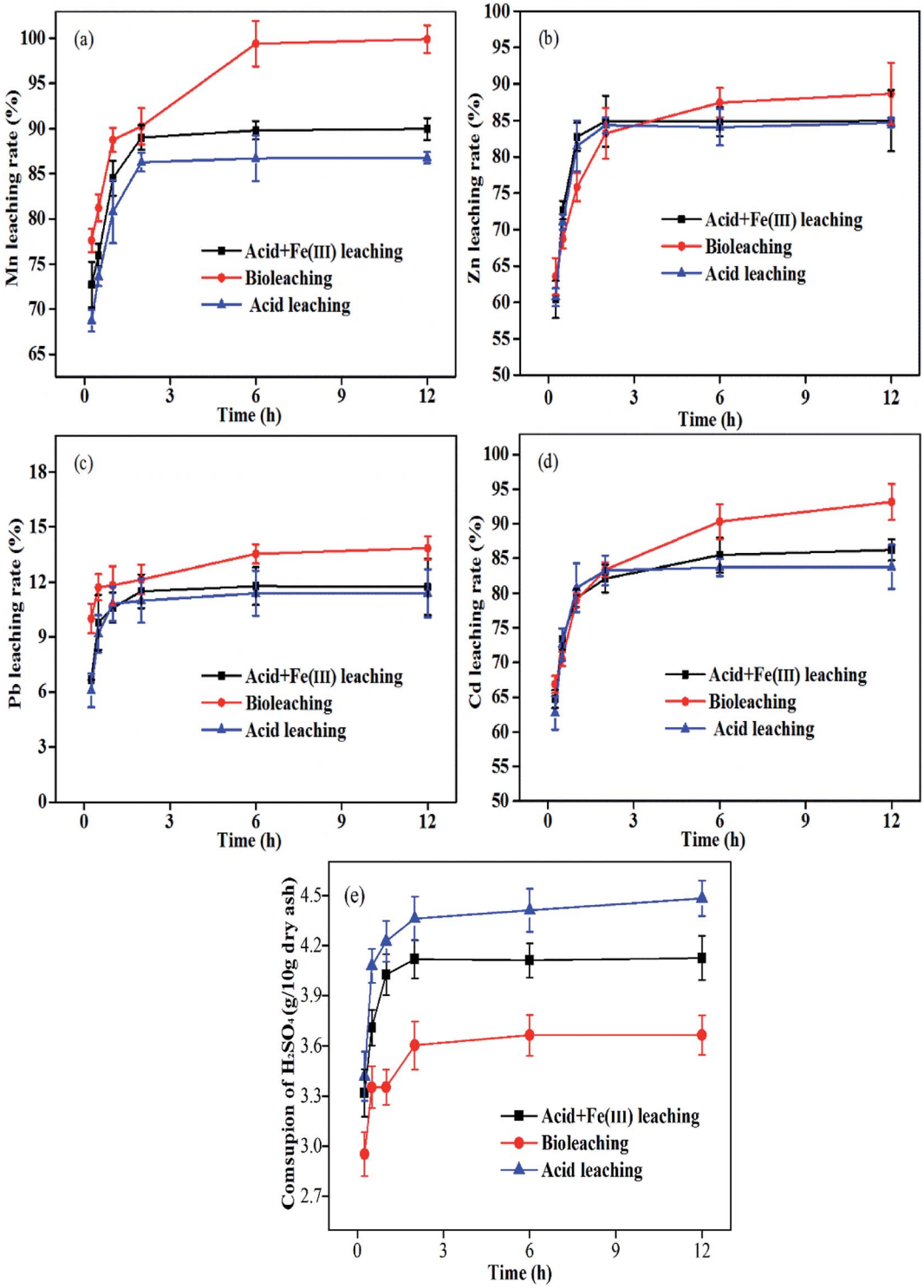

Fig. 4 Comparison of acid leaching, 'Acid + Fe(III)' leaching and bioleaching in stirred tank reactors: leaching rates of Mn (a), Zn (b), Pb (c) and Cd (d), and the total H_2SO_4 consumption (e).

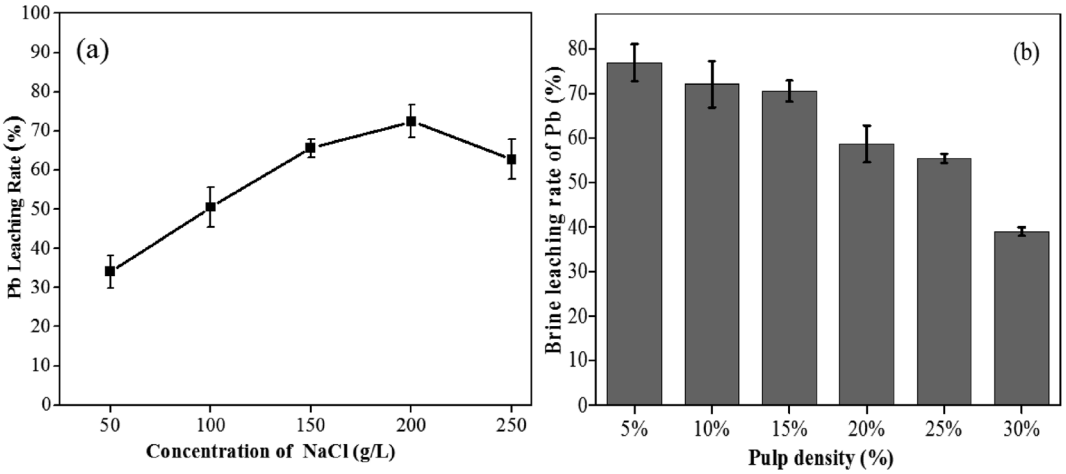

Fig. 5 Effects of different NaCl concentrations (a) and pulp densities (b) on Pb leaching from bioleached residues at 2 h.

In addition, the removal of lead from bioleached residues also depends on pulp density. According to Fig. 5b, it can be found that more than 70% of Pb is released into solution at a pulp density of 15% (w/v). Increasing the pulp density decreased the leaching rate of Pb, which is consistent with the reported phenomenon of brine leaching for lead-zinc mine tailings or hydrometallurgical residues.[17,36] This may be due to the reduced amount of Cl^- in the leaching solution and the generation of sodium jarosite hindering the interaction between the solid and the liquid.[37]

3.6 Exploration of the mechanism for the release of metals

3.6.1 Chemical simulation of Zn, Cd, Mn and Pb extraction by bioleaching. To simulate bioleaching in the ferrous-oxidation bioleaching system and analyze the contributions of H^+ and Fe(III) to tested metal release, this experiment set up two chemical acid leaching processes by using sulfuric acid and ferric sulfate (6 g L^{-1} Fe(III)) at pH 1.8. The variations in leaching rate of heavy metals and metal speciation under three different processes over time are shown in Fig. 4 and Fig. 6, respectively.

Under the acid leaching conditions, the dissolution of Zn, Cd, Mn and Pb increased quickly within the first 3 hours, and then reached a maximum release of around 85.2% (Zn), 83.8% (Cd), 86.8% (Mn) and 11.4% (Pb) within 12 h. Unlike acid leaching, only a modest increase in target metal release was observed in 'Acid + Fe(III)' leaching and 'Acid + Fe(III) + Iron-oxidizing consortium' leaching, respectively. It can be found that acid dissolution by H^+ accounted for most of the target metal release from plant ash. Thus, the H^+ mechanism was one of the main mechanisms for the target metals (Zn, Cd, Mn and Pb) leaching. Besides, in the simulated chemical leaching of 'Acid + Fe(III)', the introduction of Fe(III) into the solution increased the release rates to 85.0% (Zn), 86.2% (Cd), 90.0% (Mn) and 11.7% (Pb), which mainly benefited from the oxidation reaction of ferric iron.[38] In contrast, bioleaching with the iron-oxidizing consortium further improved the metal extraction to 99.9% (Mn), 88.7% (Zn), 93.2% (Cd) and 13.8% (Pb) with less consumption of H_2SO_4 (Fig. 4e), which showed a unique advantage in plant ash.

In addition, the changes in multi-metal speciation *via* three different leaching systems are shown in Fig. 6. Compared to the metal speciation distribution in raw ash in Table 2, H^+ accounted for most of the Mn, Cd and Zn extraction, which mainly existed in the exchangeable fraction and the oxidizable fraction. But the percentages of oxidizable fraction and residual fraction for Zn were both significantly higher than those of Mn and Cd, thereby causing a difficulty in dissolving Zn. Overall, the final fractions of extracted Zn, Cd, Mn and Pb were similar in the acid leaching and 'Acid + Fe(III)' leaching. Whereas, in the bioleaching system, the oxidizable fraction, exchangeable fraction and reducible fraction for the target metals were less observed in bioleached residues, especially for the key metal Zn. Therefore, the iron-oxidation bioleaching system showed a better performance than the two chemical leaching systems

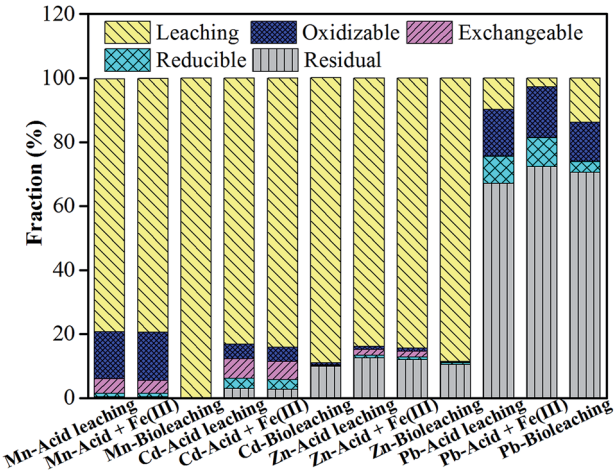

Fig. 6 The distribution of heavy metal speciation in three residues after acid leaching, 'Acid + Fe(III) leaching' and bioleaching, respectively.

Table 2 Element speciation in different fractions using a modified BCR method

Step	Fraction	Mn (%)	Zn (%)	Cd (%)	Pb (%)
1	Exchangeable	14.07%	16.21%	33.39%	0.68%
2	Reducible	0.89%	0.98%	3.02%	0.91%
3	Oxidizable	80.07%	73.40%	57.02%	81.48%
4	Residual	4.97%	9.41%	6.57%	16.93%

with more bioleaching mechanisms than dissolution by H^+ and Fe(III).

3.6.2 XRD, FTIR and SEM analyses and kinetics of bioleaching. As shown in the XRD patterns from Fig. 7a, the main minerals of SiO_2, KCl and $CaCO_3$ were detected in raw plant ash. After bioleaching, the diffraction peaks of calcite ($CaCO_3$) disappeared, the peak of potassium chlorate (KCl) was weak, but silicon was strengthened in the bioleached residues, which suggested that the crystal structure of plant ash was destroyed by bioleaching with iron-oxidizing bacteria. Meanwhile, the secondary minerals, mainly including anglesite ($PbSO_4$) and jarosite ($KFe_3(SO_4)_2(OH)_6$) appeared in the bioleached residues. These results indicated that the formation of $PbSO_4$ led to the low bioleaching of Pb, and the presence of jarosite actually affected the kinetics or dissolution of multi-metals (for example, a high concentration of Fe^{2+}).[39]

The results of the FTIR spectrum in Fig. 7b again indicated the appearance of the band of SO_4^{2-} related to $PbSO_4$ near 1087 cm^{-1} in the bioleached residues.[40] The original band of O–H at 3135 cm^{-1} disappeared, but the O–H group appeared at around at 3418 cm^{-1}, due to the O–H vibration in water molecules in the leaching ash. The strong absorption bands near 3135 cm^{-1}, 1462 cm^{-1}, 672 cm^{-1} and 618 cm^{-1} corresponding to C–H, C–O, CO_3^{2-} and M–O disappeared, indicating the dissolution of carbonate and the release of metals. The peaks near 780 cm^{-1} caused by Si–O–Si inter-tetrahedral bridge bonds became stronger than those for raw ash.[41] Furthermore, SEM images in Fig. 7c and d showed that, compared to raw ash, the surface of the bioleached residue was severely etched and covered by a porous layer, which was caused by bacterial action and attack by Fe(III) and H^+.[35]

To further uncover the metal release from plant ash, a shrinking core model was applied in this study to describe the bioleaching kinetics in plant ash, due to reduction in the mass and particle size of the leaching residues occurring during leaching. As shown in Fig. 1–4, the rates of metal

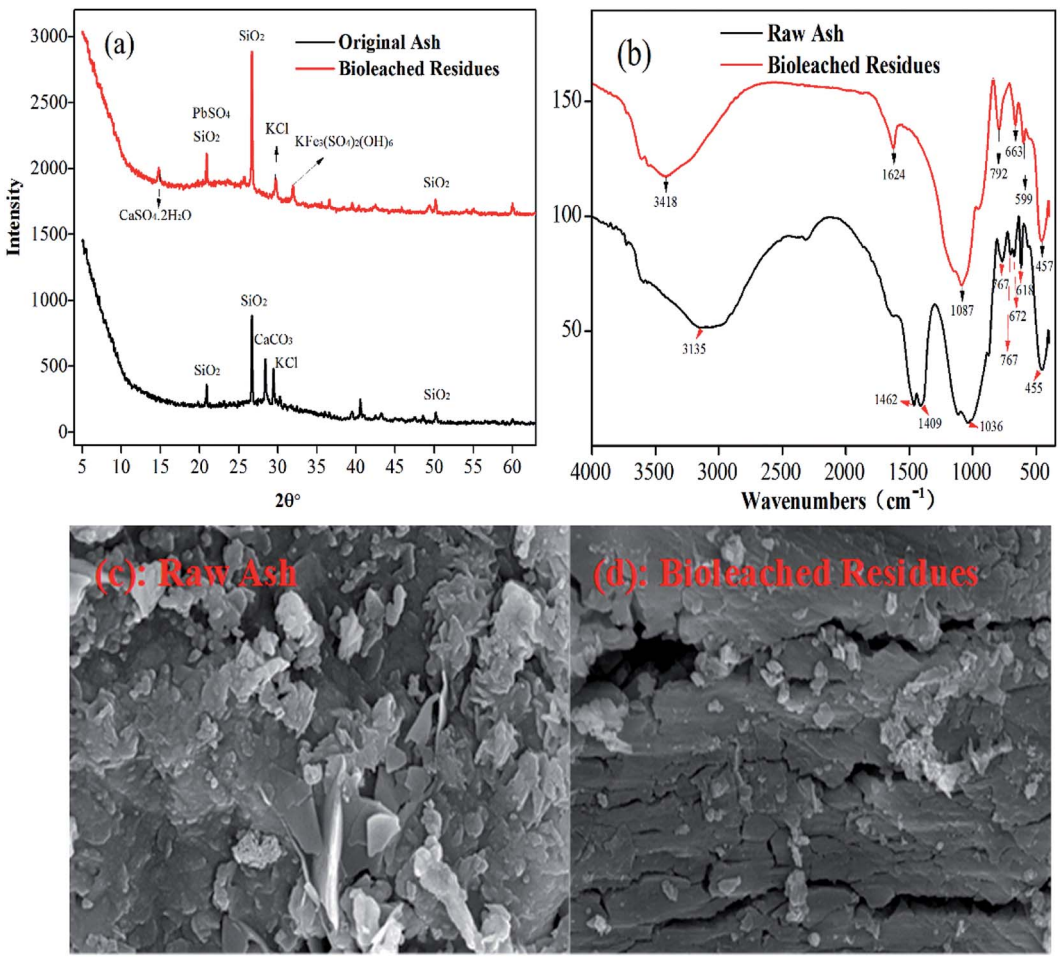

Fig. 7 Characterization of raw ash and bioleached residues: (a) XRD spectrograms; (b) FTIR spectra and (c and d) SEM images.

bioleaching decreased in the order Mn > Cd > Zn. It can be concluded that Zn was the most difficult to release and was remarkably influenced by Fe(II) concentration, pH, and pulp density. Thus, the kinetic characteristics of Zn leaching were investigated by the shrinking core model. Fig. 8 shows that the kinetics of bioleaching Zn under different Fe(III) concentrations, pH and pulp density fitted the shrinking core model well (R^2 ranging from 0.945 to 0.992) from 0 to 12 h with no lag phase. This result benefited from the two-step bioleaching strategy used for plant ash, which differs from the lag phase of 5 days in the bioleaching kinetics from mine tailings.[42] The data set indicated that the interfacial transfer and diffusion across the product layer controlled the dissolution kinetics of Zn bioleaching from plant ash. This is likely to be attributable to the relatively higher metal leaching in the bioleaching process and the low porosity of the dewatered ash during the deposition of the metals.

3.7 Environmental risk evaluation of plant ash

The remaining metals in the residues would lead to deleterious consequences for the product and pose a potential threat to human health. In addition, there is great bias against the use of this kind of ash as a material with a high risk of contaminant release. Hence, it is essential to assess the risk and toxicity of heavy metals in plant ash before landfilling or reuse.

According to the Soil Environmental Quality Standard implemented in China (GB/15618/2018) in Table 3, the results indicated that the heavy metals Zn, Cd and Pb in the raw plant ash exceeded the criteria, but after bioleaching, the contents of Zn and Cd in the residues were below the risk values for Zn of 200 mg kg^{-1} and for Cd of 0.3 mg kg^{-1}, while the Pb content was 254.7 mg kg^{-1}, higher than the risk value of 80 mg kg^{-1} (Table 3). Moreover, through brine leaching, the content of Pb in the residues was reduced to only 73.34 mg kg^{-1}, which was below the risk value of 80 mg kg^{-1}.

In addition, the leaching toxicity of the raw ash and leached residues were evaluated by toxicity characteristic leaching procedure (TCLP) tests in Table 4. Before leaching, Zn, Cd, Mn, Cr and Ni in the leachate were much higher than the Chinese regulatory limit (Chinese National Standard, GB8978-1996), and the dissolution of Ni, Pb and Cd also breached the Chinese regulatory limit for landfill disposal (Chinese National Standard, GB16889-2008). Thus, the untreated plant ash had high environmental toxicity. After biological treatment, except for Pb content at around

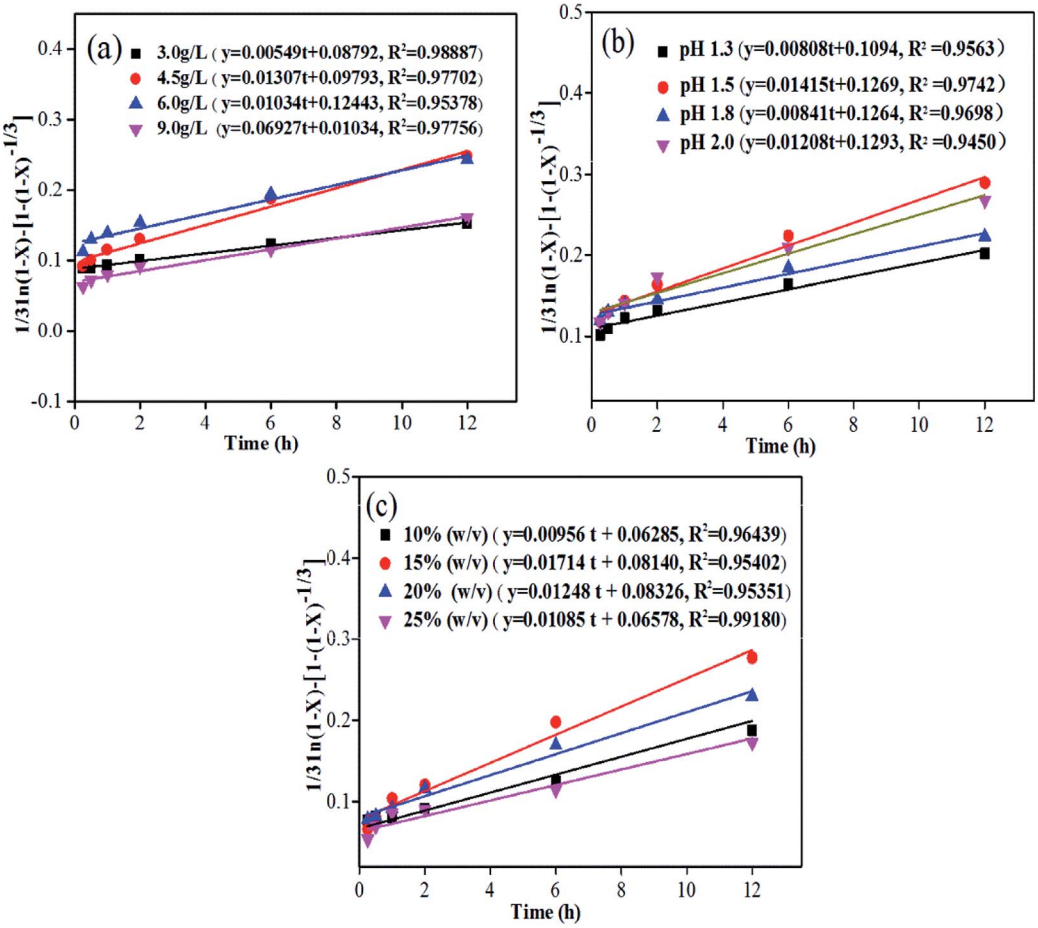

Fig. 8 Dissolution-controlled model for bioleaching of Zn from ash: (a) different Fe(II) concentrations; (b) different pH values; (c) different pulp densities.

Table 3 Major elemental content in the residues before and after bioleaching

Item	Plant ash (mg kg^{-1})	Bioleached residue (mg kg^{-1})	Final residue (mg kg^{-1})	Risk value[b] (mg kg^{-1})
pH[a]	10.5 ± 0.3	2.0 ± 0.2	1.5 ± 0.2	—
Mn	3888.0 ± 60.3	303.0 ± 6.3	276.0 ± 6.2	—
Zn	2278.0 ± 52.3	169.0 ± 2.5	163.0 ± 2.4	200
Cd	5.1 ± 0.4	0.20 ± 0.03	0.19 ± 0.02	0.30
Pb	187.9 ± 6.3	254.7 ± 6.2	73.3 ± 1.4	80
Cr	28.0 ± 1.3	28.6 ± 1.4	28.8 ± 1.3	250
Cu	86.6 ± 4.4	38.4 ± 0.9	34.5 ± 0.4	50
Ni	81.5 ± 3.1	17.4 ± 1.2	17.5 ± 1.3	60
Fe	13 360.0 ± 230.9	24 660.0 ± 310.3	24 571.0 ± 313.4	—
K	15 300.0 ± 100.6	10 290.0 ± 186.3	10 248.0 ± 188.7	—
Ca	42 170.0 ± 401.8	2264.0 ± 48.4	2213.0 ± 53.2	—
Na	937.0 ± 16.3	249.8 ± 2.4	354.8 ± 4.0	—

[a] The pH value: based on Chinese Standard of Solid Waste – Glass Electrode Test Method of Corrosivity (GB/T 15555.12-1995). [b] The risk value referred to Soil environmental quality – Risk control standard for soil contaminated of agricultural land of China (GB 15618-2018).

Table 4 Toxicity assessment tests of raw ash and residues before and after leaching

Item	Raw plant ash (mg L^{-1})	Bioleached residue (mg L^{-1})	Final residue (mg L^{-1})	[a]Threshold limit (mg L^{-1})	[b]Threshold limit (mg L^{-1})
Pb	0.95 ± 0.02	0.75 ± 0.01	—	5	1
Zn	15.26 ± 0.13	0.29 ± 0.01	0.28 ± 0.02	100	5
Cd	0.19 ± 0.01	—	—	1	0.1
Ni	1.36 ± 0.11	0.32 ± 0.03	0.30 ± 0.02	5	1
Cu	1.32 ± 0.04	—	—	100	2
Mn	25.21 ± 0.31	—	—	NL	5
Cr	2.50 ± 0.03	—	—	5	1.5

[a] According to the Standard for Pollution Control on the Landfill Site of Municipal Solid Waste (Chinese National Standard GB 16889-2008). [b] According to the Standard for Industrial Wastewater Emission (Chinese National Standard, GB8978-1996).

0.75 mg L^{-1}, only a small amount of heavy metals was detected in the residues. Subsequently, with the employment of brine leaching for bioleached residues, there was no lead detected in the final leach residues. These data indicated that the treated residue was nonhazardous and could be safely utilized in commercial products of construction materials for roads and buildings. Thus, the two-stage strategy almost puts an end to the possibility of secondary pollution of heavy metals for plant ash.

4 Conclusions

Plant ash contains SiO_2, KCl, $CaCO_3$ and partly amorphous Mn, Zn, Cd and Pb, which was remarkably different to that reported from fly ash and would pose threats to the environment. This study proposed a cleaner strategy of bioleaching combined with brine leaching. Bioleaching rates of 88.7% (Zn), 93.2% (Cd), 99.9% (Mn) and 13.8% (Pb) were achieved under optimum conditions of Fe(II) concentration 6.0 g L^{-1}, pH 1.8 and pulp density 15% (w/v). Subsequently, the introduction of brine leaching using 200 g L^{-1} NaCl significantly increased Pb recovery to 70.6% under 15% (w/v) pulp density conditions, thereby ultimately achieving deep recovery of all metals. An investigation of the mechanism revealed that H^+ attack and microorganisms were the dominant mechanism for Zn, Cd and Mn leaching. Risk assessment tests indicated that leached residues could be safely reused as nonhazardous materials. These findings demonstrated the feasibility and efficiency of a two-stage leaching strategy and provide new insight into multi-metal removal from plant ash.

Conflicts of interest

There are no conflicts to declare.

Acknowledgements

This work was supported by the National key R & D Program Task, China (2017YFD0801304).

References

1 M. N. V. Prasad and H. M. D. O. Freitas, *Electron. J. Biotechnol.*, 2003, **6**, 189–198.
2 C. H. Lam, A. W. Ip, J. P. Barford and G. McKay, *Sustainability*, 2010, **2**, 1943–1968.

3 A. Sas-Nowosielska, R. Kucharski, E. Małkowski, M. Pogrzeba, J. Kuperberg and K. J. E. P. Kryński, *Environ. Pollut.*, 2004, **128**, 373–379.
4 C. Zhou, S. Ge, H. Yu, T. Zhang, H. Cheng, Q. Sun and R. Xiao, *J. Cleaner Prod.*, 2018, **177**, 699–707.
5 D. Houben, L. Evrard and P. Sonnet, *Biomass and Bioenergy*, 2013, **57**, 196–204.
6 A. Sas-Nowosielska, R. Kucharski, E. Malkowski, M. Pogrzeba, J. M. Kuperberg and K. Krynski, *Environ. Pollut.*, 2004, **128**, 373–379.
7 S. Lu, Y. Du, D. Zhong, B. Zhao, X. Li, M. Xu, Z. Li, Y. Luo, J. Yan and L. Wu, *J. Environ. Sci. Technol.*, 2012, **46**, 5025–5031.
8 A. Liu, F. Ren, W. Y. Lin and J.-Y. Wang, *Int. J. Sustainable Built Environ.*, 2015, **4**, 165–188.
9 C. Li, F. Xie, Y. Ma, T. Cai, H. Li, Z. Huang and G. Yuan, *J. Hazard. Mater.*, 2010, **178**, 823–833.
10 K. Anastasiadou, K. Christopoulos, E. Mousios and E. Gidarakos, *J. Hazard. Mater.*, 2012, **207–208**, 165–170.
11 D. W. Kirk, C. C. Chan and H. Marsh, *J. Hazard. Mater.*, 2002, **90**, 39–49.
12 C. Kersch, G. F. Woerlee and G. J. Witkamp, *Ind. Eng. Chem. Res.*, 2004, **43**, 190–196.
13 M. K. Jha, J.-c. Lee, M.-s. Kim, J. Jeong, B.-S. Kim and V. Kumar, *Hydrometallurgy*, 2013, **133**, 23–32.
14 T. Y. Gu, S. O. Rastegar, S. M. Mousavi, M. Li and M. H. Zhou, *Bioresour. Technol.*, 2018, **261**, 428–440.
15 S. Feng, H. Yang and W. Wang, *RSC Adv.*, 2015, **5**, 98057–98066.
16 M. Ye, P. Yan, S. Sun, D. Han, X. Xiao, L. Zheng, S. Huang, Y. Chen and S. Zhuang, *Chemosphere*, 2017, **168**, 1115–1125.
17 E. Hsu, K. Barmak, A. C. West and A.-H. A. Park, *Green Chem.*, 2019, **21**, 919–936.
18 P. Rasoulnia and S. M. Mousavi, *RSC Adv.*, 2016, **6**, 9139–9151.
19 P. P. Bosshard, R. Bachofen and H. Brandl, *Environ. Sci. Technol.*, 1996, **30**, 3066–3070.
20 R. Blissett and N. Rowson, *Fuel*, 2012, **97**, 1–23.
21 F. Farahmand, D. Moradkhani, M. S. Safarzadeh and F. Rashchi, *Hydrometallurgy*, 2009, **95**, 316–324.
22 F. Giebner, S. Kaschabek, S. Schopf and M. Schlömann, *Miner. Eng.*, 2015, **79**, 169–175.
23 Y. Wang, W. Zeng, G. Qiu, X. Chen and H. Zhou, *Appl. Environ. Microbiol.*, 2014, **80**, 741–750.
24 F. Pourhossein and S. M. Mousavi, *J. Hazard. Mater.*, 2019, **378**, 120648.
25 K. Nemati, N. K. A. Bakar, M. R. Abas and E. Sobhanzadeh, *J. Hazard. Mater.*, 2011, **192**, 402–410.
26 W. Zhou, L. Zhang, J. Peng, Y. Ge, Z. Tian, J. Sun, H. Cheng and H. Zhou, *Chemosphere*, 2019, **232**, 345–355.
27 Y. Xie, G. Lu, C. Yang, L. Qu, M. Chen, C. Guo and Z. Dang, *PLoS One*, 2018, **13**, e0190010.
28 D. E. Rawlings, D. Dew and C. du Plessis, *Trends Biotechnol.*, 2003, **21**, 38–44.
29 J. J. Plumb, R. Muddle and P. D. Franzmann, *Miner. Eng.*, 2008, **21**, 76–82.
30 B. Bayat and B. Sari, *J. Hazard. Mater.*, 2010, **174**, 763–769.
31 A. Ahmadi, M. Schaffie, J. Petersen, A. Schippers and M. J. H. Ranjbar, *Hydrometallurgy*, 2011, **106**, 84–92.
32 H. Y. Wu and Y. P. Ting, *Enzym. Microb. Technol.*, 2006, **38**, 839–847.
33 L. Wang, W. N. Mu, H. T. Shen, S. M. Liu and Y. C. Zhai, *Int. J. Miner., Metall. Mater.*, 2015, **22**, 460–466.
34 M. Ye, G. Li, P. Yan, L. Zheng, S. Sun, S. Huang, H. Li, Y. Chen, L. Yang and J. Huang, *Sep. Purif. Technol.*, 2017, **183**, 366–372.
35 A. Ruşen, A. S. Sunkar and Y. A. Topkaya, *Hydrometallurgy*, 2008, **93**, 45–50.
36 Z.-h. Guo, F.-k. Pan, X.-y. Xiao, L. Zhang and K.-q. Jiang, *Trans. Nonferrous Metals Soc. China*, 2010, **20**, 2000–2005.
37 B. Bayat and B. Sari, *J. Hazard. Mater.*, 2010, **174**, 763–769.
38 Q. Liu, Y. Zhao and G. Zhao, *Hydrometallurgy*, 2011, **110**, 79–84.
39 L. Reyes-Bozo, M. Escudey, E. Vyhmeister, P. Higueras, A. Godoy-Faúndez, J. L. Salazar, H. Valdés-González, G. Wolf-Sepúlveda and R. Herrera-Urbina, *Miner. Eng.*, 2015, **78**, 128–135.
40 P. Rasoulnia, S. M. Mousavi, S. O. Rastegar and H. Azargoshasb, *Waste Manag.*, 2016, **52**, 309–317.
41 M. Ye, G. Li, P. Yan, J. Ren, L. Zheng, D. Han, S. Sun, S. Huang and Y. Zhong, *Chemosphere*, 2017, **185**, 1189–1196.
42 S. O. Rastegar, S. M. Mousavi, S. A. Shojaosadati and R. S. Mamoory, *Hydrometallurgy*, 2015, **157**, 50–59.